J. Enzyme Inhibition, 1988, Vol. 13, pp. 11–29
Reprints available directly from the publisher
Photocopying permitted by license only

THE MECHANISM OF BINDING OF LOW-MOLECULAR-WEIGHT ACTIVE SITE INHIBITORS TO HUMAN α-THROMBIN

THOMAS NILSSON[a,†], ÅSA SJÖLING-ERICKSSON[a] and JOHANNA DEINUM[b,*]

[a] *Department of Biochemistry and Biophysics, University of Göteborg, Medicinaregatan 4D, S-413 90 Göteborg, Sweden;* [b] *Astra Hässle AB, Biochemistry, Preclinical R & D, S-431 83 Mölndal, Sweden*

(Received 24 April 1997; In final form 21 July 1997)

The thrombin inhibitors argatroban, efegatran, NAPAP, CH 1091, CH 248, inogatran and melagatran have been characterised with respect to their mechanism of binding to human α-thrombin. Stopped-flow spectrophotometry was used to follow thrombin-catalysed hydrolysis of the chromogenic substrate S-2238 in the presence of inhibitors. The rate of onset or decay of inhibition was evaluated using progress curve analysis. It was possible to obtain apparent association and dissociation rate constants from the dependence of the rates on the inhibitor concentrations. Inhibition constants calculated from the association and dissociation rate constants were in good agreement with those calculated from steady-state rates. The binding of 6 inhibitors was also monitored directly using stopped-flow spectrofluorimetry when two kinetic components were found with all inhibitors. The faster component accounted for the largest part of the change in the intrinsic fluorescence of thrombin induced by inhibitor binding and was dependent on the inhibitor concentration. The slower component was independent of the concentration of the inhibitor. The concentration dependence of the faster component was linear with the compounds argatroban, NAPAP, CH 1091 and melagatran and hyperbolic with the compounds CH 248 and inogatran. The values of the apparent second-order rate constants at pH 7.4 and 37°C range from slow to rapid binding in the interval $16-78 \times 10^6\,M^{-1}s^{-1}$, which is somewhat higher than $1-34 \times 10^6\,M^{-1}s^{-1}$ obtained from progress curve analysis of the onset of inhibition.

The present results support a mechanism that includes rearrangement of a weak initial thrombin–inhibitor complex towards a tighter complex. Moreover, at least one additional step is required in the mechanism. In this model, the rate-limiting step for the binding of the inhibitor at concentrations in the nanomolar range depends on the primary interaction between the inhibitor and native thrombin.

* Corresponding author. Tel.: +46 31 7761592. Fax: +46 31 7763736.
E-mail: johanna.deinum@hassle.se.astra.com.
† Present address: University of Karlstad, Dept. Natural Sci., S-651 88 Karlstad, Sweden.

Keywords: Thrombin; Tight-binding; Progress phase analysis; Conformational change; Fluorescence spectroscopy; Enzyme inhibitor

Abbreviations: argatroban – (*R*,*S*)Tmq-SO_2-Arg-(*R*)Pic(4-(*R*)Me); Aze – L-azetidine-2-carboxylic acid; BSA – bovine serum albumin; Cgl – cyclohexylglycine; CH 1091 – HOOC-CH_2-(*R*)Cha-Pro-(*R*,*S*)Arg[CH_2-O-CH_2-CF_3]; CH 248 – H-(*R*)Cha-Pro-Arg[$CH_2OCH_2CF_3$]; Cha – cyclohexylalanine; efegatran – Me-(*R*)Phe-Pro-Arg[H]; Hepes – *N*-[2-hydroxyethyl] piperazine-*N*′-[2-ethane-sulphonic acid]; inogatran – HOOC-CH_2-(*R*)Cha-Pic-Nag; melagatran – HOOC-CH_2-(*R*)Cgl-Aze-Pab; Nag – noragmatine; NAPAP – *N*″-(2-naphthylsulphonylglycyl)-DL-*p*-amidino-Phe-piperidide; Pab – para-amidino-benzylamine; PEG – polyethylene glycol 6000; Pic – L-piperidine-2-carboxylic acid]; S-2238 – H-(D)-Phe-L-Pip-L-Arg-*p*-nitroanilide · HCl; Tmq – 3-methyl-1,2,3,4-tetrahydro-8′-quinolinyl.

INTRODUCTION

The trypsin-like serine protease thrombin (EC 3.3.21.5) has a central role in the regulation of thrombosis and haemostasis, by converting fibrinogen into clottable fibrin. The efficiency of thrombin inhibitors as antithrombotic drugs depends both on their affinity for the target and their rate of binding.[1] It is therefore desirable to include kinetic studies of inhibitor binding to thrombin in the characterisation of compounds developed as thrombin inhibitors. Classical reversible enzyme inhibition is characterised by rapid equilibrium between the enzyme and inhibitor and the enzyme–inhibitor complex, with the equilibrium dissociation constant, K_i. Furthermore, inhibitors can be slow binding, such that steady-state is not reached during the initial reaction with the substrate.[1–3] It is clear that the definition "slow" or "rapid" binding is relative. The reason for slow inhibition, although dependent on the reaction mechanism,[2] is generally a low second-order association rate constant, k_{on},[1,4] but it can also depend on a low value for k_{off}, as found for the thrombin inhibitors of the boroarginine type.[5,6]

In the present study, we have characterised the binding properties of different active site inhibitors, see Figure 1, with regard to inhibition of thrombin. It was found that several potent thrombin inhibitors can be classified as moderately slow binding, competitive, reversible thrombin inhibitors. For these compounds, we were able to determine the k_{on} and k_{off} for the formation of the inhibited enzyme, using stopped-flow spectrophotometry for monitoring progress curves. The use of this rapid technique allowed the characterisation of the binding kinetics of the compounds argatroban, CH 1091, CH 248, inogatran and melagatran on the time scale of seconds. Progress curve analysis is, however, an indirect method that

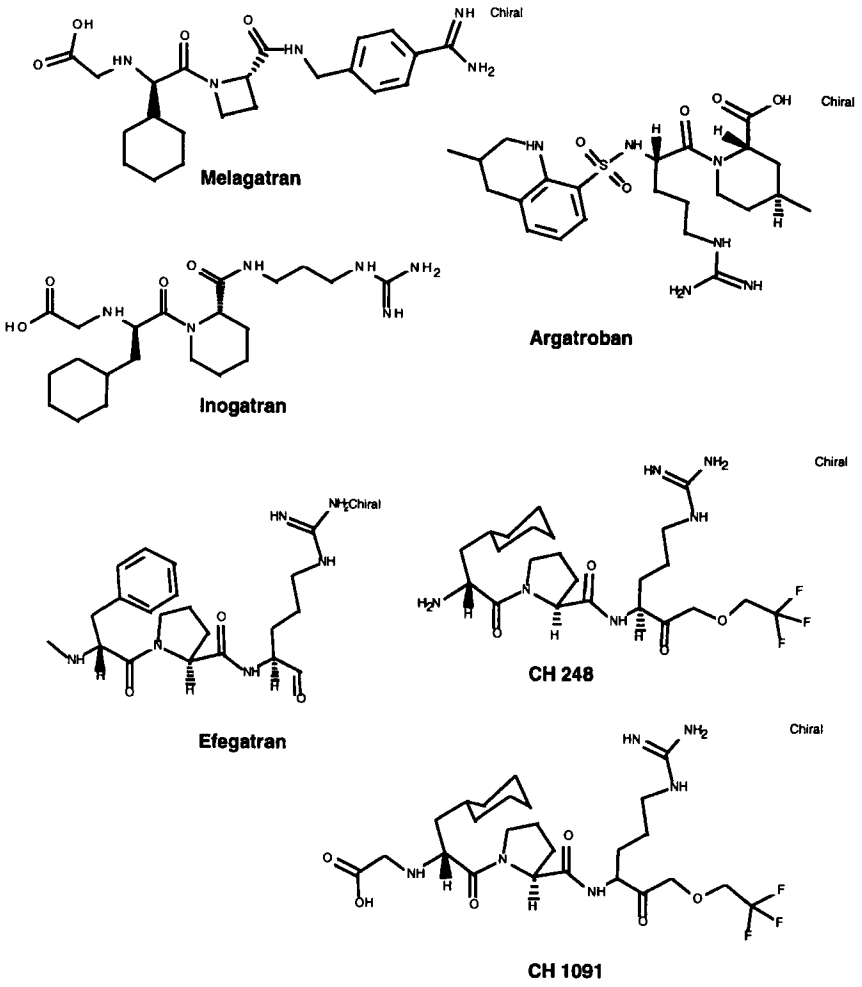

FIGURE 1 Specific inhibitors of thrombin.

relies on monitoring changes in the rate of thrombin-catalysed hydrolysis of a chromogenic substrate. A more direct approach was therefore used for the study of inhibitor binding, applying the technique of stopped flow fluorescence. When the present study was in progress Parry *et al.*[7] also showed that binding of a series of inhibitors to thrombin is accompanied by a change in the intrinsic fluorescence of the protein.

The aim of the present work was to investigate these techniques to characterise and to compare binding of different active site inhibitors to human α-thrombin. All compounds tested induced a fluorescence change in

thrombin sufficiently large to allow the use of stopped-flow with fluorescence detection to monitor binding. With this technique it was possible to detect two kinetic components with all inhibitors. The faster component, which accounted for the larger part of the fluorescence change, was found to be linearly dependent on the inhibitor concentration with the inhibitors argatroban, NAPAP, melagatran and CH 1091, and hyperbolically dependent on the inhibitor concentration with inogatran and CH 248. The rate constants found for the slower kinetic component did not depend appreciably on the concentration of the inhibitor. The hyperbolic concentration dependence of the observed rate constant for the rapid component indicates that the initial binding takes places in two steps. The results are therefore consistent with inhibitor binding taking place in at least three steps: a relatively weak initial binding in two steps, followed by a conformational change that leads to tighter binding.

MATERIALS AND METHODS

Chemicals

BSA (bovine albumin fraction V) was from ICN Biomedicals Ltd. (High Wycombe, Bucks, Great Britain). All other chemicals were reagent grade. All solutions were made with Super-Q Plus water, Millipore Co. (Bedford, MA, USA).

Buffers

The pH of the buffers was adjusted to 7.4 at 20°C. The buffer used in the fluorescence measurements was 0.05 M *N*-[2-hydroxyethyl] piperazine-*N'*-[2-ethane-sulphonic acid] (Hepes) containing 0.15 M NaCl and 0.1% polyethylene glycol 6000 (PEG). In the pre-steady-state experiments the buffer contained 0.1% (w/v) BSA, instead of PEG. The buffer used in the steady-state measurements, performed with the Cobas Bio, consisted of 0.05 M Tris and 0.1% BSA, and the ionic strength was adjusted to 0.15 M with NaCl.

Inhibitors

N^{α}-(2-naphthylsulphonylglycyl)-DL-*p*-amidino-Phe-piperidide (NAPAP) was obtained from Sigma Chemical Company (St. Louis, MO, USA). (*R*,*S*)Tmq-SO_2-Arg-(*R*)Pic(4-(*R*)Me) (argatroban) was obtained from

Mitsubishi Kasei Dai i Chi (Tokyo, Japan) as a 0.98 mM solution in water containing sorbitol. The enriched epimers of CH 1091 (HOOC-CH_2-(*R*)Cha-Pro-(*R*,*S*) Arg-CH_2-O-CH_2-CF_3) (*S*)-CH 1091 and (*R*)-CH 1091 and the compounds (H-(*R*)Cha-Pro-Arg-CH_2-O-CH_2-CF_3) (CH 248) were synthesised at Ferring Research (Chilworth, UK). Me-(*R*)Phe-Pro-Arg-H · H_2SO_4 (efegatran, Patent Application US4703036), HOOC-CH_2-(*R*)Cha-Pic-Nag (inogatran, Patent Application WO9311152-A1) and HOOC-CH_2-(*R*)Cgl-Aze-Pab (melagatran, Patent Application WO9429336-A) were synthesised at Astra Hässle AB (Mölndal, Sweden). The structures of the inhibitors are presented in Figure 1. The inhibitors were diluted in 0.12 M NaCl in sterile filtered water to a stock solution, filtered through a 0.22 μm sterile filter (Millipore Co., Bedford, USA) and stored in aliquots at −20°C. All further dilutions were made with the buffer used in the particular assay.

Thrombin Solutions

Lyophilised human α-thrombin (T6759; lot 103H9308) was obtained from Sigma Chemical Company (St. Louis, MO, USA). For the steady-state assays, thrombin was reconstituted in the appropriate buffer to approximately 0.4 μM. For the pre-steady-state kinetics, thrombin was reconstituted with 0.15 NaCl containing 0.1% (w/v) BSA. For the fluorescence studies, thrombin was reconstituted to produce a 10 μM stock solution in 0.05 M sodium citrate buffer with 0.15 M NaCl at pH 6.5. All stock solutions of thrombin were stored in 1 ml Eppendorf tubes at −70°C. On the day of the experiment, the solutions were rapidly thawed at 37°C and kept on ice until the working solution was prepared by dilution with the buffer.

Chromogenic Substrate

The thrombin substrate S-2238, H-(D)-Phe-L-Pip-L-Arg-*p*-nitroanilide · HCl (Chromogenix, Mölndal, Sweden), was dissolved in water, 25 g/L, to a nominal concentration of 40 mM. The stock solution was further diluted with assay buffer to final concentrations of 0.16, 0.24 and 0.50 mM for the steady-state experiments, unless otherwise indicated, or 1.18 or 1.5 mM for the stopped-flow experiments. The concentration of S-2238 used in the stopped-flow experiments was measured from the absorbance at 316 nm and $\varepsilon_{316} = 12.7 \cdot (\text{mM})^{-1}\,\text{cm}^{-1}$.[8]

We determined a K_M of 5.4 μM for thrombin for S-2238 in the buffer used for the stopped-flow experiments (Hepes buffer at pH 7.4, at 37°C)

from a Hanes plot, using the average values obtained for six different substrate concentrations (4.5–45 μM) at three different enzyme concentrations (0.7, 1.4 and 2.1 nM) (not shown). The value 5.4 μM was used throughout in the calculation of k_{on} and k_{off} and for the calculation of K_i in the pre-steady-state phase. It has been shown before that the K_M is extremely sensitive to changes in the buffer conditions.[8] This may explain why this value is slightly lower than that reported by the manufacturer of the chromogenic substrate (7 μM at 37°C, in Tris-buffer at pH 8.3, with an ionic strength of 0.15 M), but higher than reported in the absence of BSA with a mixture of Tris and Hepes buffer.[8,9]

Optical Absorbance Measurements

An LKB Ultrospec spectrophotometer from LKB-Pharmacia Biotechnology (Uppsala, Sweden) was used for the determination of the K_M of S-2238. The data collection software used was LKB 4073-420, Reaction Rate Software from LKB Biochrom (Uppsala, Sweden). Absorbance spectra of the protein solutions were recorded with a Shimadzu UV-160 and a Shimadzu UV-3000 from Shimadzu Co. (Tokyo, Japan). The Cobas Bio Centrifugal Spectroanalyzer was from Roche (Basel, Switzerland). Kinetic measurements, using 1 : 1 mixing, were made with an SX17MV stopped-flow spectrophotometer/spectrofluorimeter from Applied Photophysics (Leatherhead, UK). The dead time of the instrument was 1.1 ms, determined from the reaction between dichlorophenolindophenol and ascorbate, as described by the manufacturer. For absorbance measurements *versus* time for pre-steady-state kinetics, the wavelength was set at 405 nm.

Fluorescence Measurements

Fluorescence spectra were recorded on a Perkin Elmer LS.50B spectrofluorimeter. The excitation and emission slits were set at 10 and 5 nM, respectively. The equilibrium change in the fluorescence emission spectra was first determined by steady-state fluorescence measurements. Aliquots of a concentrated inhibitor solution were added to the thrombin solution to a maximum volume change of 0.4% and a final 20-fold excess of inhibitor over thrombin. In the kinetic fluorescence measurements, the excitation wavelength, λ_{ex}, was set at 280 nm with a bandwidth of 14 nm. Emission was detected at a right angle to the exciting light using a 320 nm cut-off filter. The temperature was 37°C throughout. In total 1000 data points were collected in each transient, and all time courses shown are averages of

18–20 individual transients. Fluorescence emission intensities are expressed in relation to the fluorescence intensity of free thrombin, determined by mixing thrombin with buffer under the same conditions. This intensity was corrected for a small background caused by scattered excitation light reaching the photomultiplier. At least five-fold molar excess of inhibitor over thrombin was used in all experiments with the stopped-flow fluorimeter. The change in fluorescence in time was analysed for different kinetic models (see below) using curve-fitting, carried out with software from Applied Photophysics, or the Igor Pro software package (Wavemetrics, Inc., Lake Oswego, OR, USA).

Determination of K_i by Steady-State Measurements

A Cobas Bio centrifugal analyser was used for these measurements. The inhibitor samples were analysed at three different initial substrate concentrations, 16, 24, or 50 μM S-2238, with 0.7 nM thrombin at 37°C. The steady-state rates at 405 nm, V_s, for thrombin were determined after the lag phase was reached, and the actual substrate concentration was calculated by correction for a decrease caused by product formation. The various concentrations of the inhibitor ($[I] \gg [E]$) were preincubated for 300 s with thrombin before substrate was added or the inhibitor was added together with the substrate solution. The value for the K_i was determined from the rate at steady-state, by non-linear regression of the steady-state function for a reversible, competitive inhibitor,[2,3] using the software package Grafit® (Erithacus Software Lim., London, UK).

Determination of K_i, k_{on} and k_{off} from Pre-Steady-State Measurements

The increase in absorbance was followed *versus* time with the stopped-flow technique during the first 2–70 seconds of product formation at 37°C. The observation time was adapted for each inhibitor. The progress phase was followed in two ways: either thrombin was preincubated with the inhibitor for 15 min at 37°C to ensure that equilibrium was established, and the reaction was initiated by mixing with the substrate; or, the substrate solution containing the inhibitor was mixed with the thrombin. The final concentrations of thrombin in the assay were chosen in the range 7–70 nM depending on the inhibitor. The inhibitor was present in the range 0.5–5 μM, with substrate concentrations in the assay of 0.5–1.5 mM, as indicated for each experiment.

Using the curve-fitting program included in the stopped-flow control program, the k_{obs} and V_s for each inhibitor concentration were determined

from the average of six or seven traces by non-linear regression, based on the Levenberg–Marquardt algorithm, using either equation (2a) or (2b). When thrombin was mixed with substrate without pre-incubation with the inhibitor, the integrated equation (1a) is valid, assuming that $[I] \gg [E]$ and $[S] \gg K_M$:

$$P_t = P_0 + V_s * t + (V_0 - V_s) * (1 - \exp(-k_{obs} * t))/k_{obs}. \qquad \text{(eq. 1a)}$$

Here P_0 and P_t represent product concentration at time t_0 and t, while V_s and V_0 represent the final steady-state and the initial velocities of the reaction, respectively, whereas k_{obs} denotes the apparent first-order rate constant for approach to steady-state. The meaning of this parameter varies with the mechanism. When the reaction was started by addition of substrate to the inhibited enzyme, regression analysis was performed applying equation (1b) for evaluation of the dissociation of the complex.[2,3]

$$P_t = P_0 + V_s * t - V_s * (1 - \exp(-k_{obs} * t))/k_{obs}. \qquad \text{(eq. 1b)}$$

With an excess of inhibitor, the initial velocity (V_0) after pre-incubation will be zero when the rate-limiting step is the binding of the inhibitor to the enzyme. From the k_{obs} values, obtained from the progress curve analysis, the steady-state kinetic parameters V_s, V_0, K_i, and the apparent values for k_{off} and k_{on} were calculated by linear regression applying the following equations. Assuming a mechanism where the attainment of equilibrium between the enzyme and enzyme–inhibitor complex[2] is rate-limiting then:

$$k_{obs} = k_{off}^{app} + k_{on}^{app} * [I]/(1 + [S]/K_M). \qquad \text{(eq. 2)}$$

From the k_{on}^{app} and the k_{off}^{app}, the K_i for the pre-steady-state phase can be calculated according to the relation: $K_i = k_{off}^{app}/k_{on}^{app}$. The K_i values in the analysis of the first minute of the progress phase have been determined from this ratio and, moreover, compared with the values for V_s obtained for a competitive inhibitor.

RESULTS

Binding of Inhibitors Monitored by Progress Curve Analysis

The substances studied in the present investigation were known from preliminary steady-state characterisation to behave as classical reversible

competitive inhibitors (not shown). The substances CH 1091 and efegatran are exceptions, since they exhibited slow binding behaviour[10,11] in the time scale of these experiments. The primary aim of the present work was to study the general mechanism of inhibitor binding. We have therefore extended the method of progress curve analysis to faster time scales using stopped-flow spectrophotometry to study the reaction[10] rates.

In Figure 2, the thrombin-catalysed hydrolysis of the chromogenic substrate S-2238 was followed in the stopped-flow apparatus in the presence of the inhibitor inogatran. The upper trace (A) was obtained on mixing thrombin with a mixture of substrate and inhibitor, the lower trace (B) on

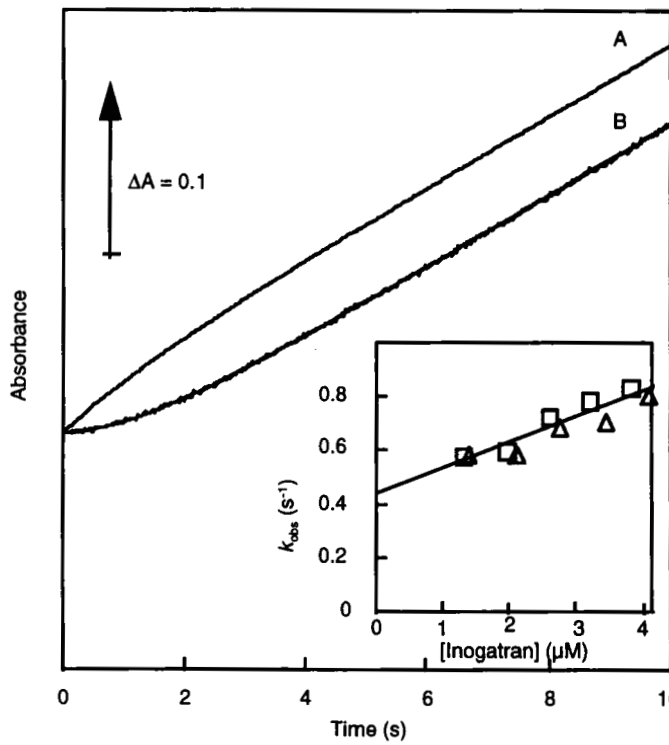

FIGURE 2 Thrombin-catalysed hydrolysis of S-2238 in the presence of inogatran. The stopped-flow technique was used to monitor product formation. The final assay contained 27 nM thrombin, 1.3 mM S-2238 and 2.76 μM inogatran in buffer A. The reaction was started without pre-incubation of thrombin with inogatran (trace A), or with pre-incubation (trace B) of thrombin with inogatran for 15 min at 37°C. The displayed traces could be fitted by non-linear regression (equations 1 and 2). The inset shows the apparent rate constant found for approach to steady-state, k_{obs} as a function of the inogatran conc. (□) = 15 min of pre-incubation of thrombin with inogatran and (△) = without pre-incubation. Each data point is the average of the k_{obs} obtained from 6 individual progress curves. The K_i = 19.4 nM was calculated from the values obtained for k_{off} and k_{on}.

TABLE I Kinetic parameters[a] for inhibitor binding obtained by progress curve analysis

Inhibitor	$k_{on}^{app} \times 10^{-6}$ ($M^{-1}s^{-1}$)	k_{off}^{app} (s^{-1})	$k_{off}^{app}/k_{on}^{app}$ (nM)	*Steady-state* K_i (nM)
Argatroban	33	0.25	7.6	10
NAPAP	NA	NA	NA	6.6[c]
Efegatran	0.85	0.002	2.3	1.8
Melagatran	12	0.05	4.2	4.1
(*S*)-CH 1091	4.6[b]	0.06	13	6.0[b]
CH 248	4.8	0.049	10.2	13
Inogatran	20	0.44	22	17

[a] In 0.05 M Hepes (pH 7.4) containing 0.1% BSA and 0.15 M with NaCl at 37°C.
[b] The value shown here was calculated assuming the *S*-epimer to be the active constituent. The experiment was performed with an 80/20 mixture of the *S*- and *R*-epimers,[11] and the actual experimental value obtained for the mixture was $k_{on}^{app} = 3.4 \times 10^6\ M^{-1}s^{-1}$.
[c] From reference [7].

mixing substrate with thrombin that had been preincubated with the inhibitor. In the absence of inhibitor, a linear trace was obtained (not shown). It was possible to fit the displayed traces to the expressions given by Morrison[2] (equations 1 and 2):

The apparent rate constants for approach to steady-state, obtained by fitting equations (1) or (2) to the data, are shown as a function of the inhibitor concentration in the inset in Figure 2. From the slope and ordinate intercept of the straight line, an apparent second-order rate constant for inhibitor binding (k_{on}^{app}) and an apparent first-order rate constant for inhibitor dissociation (k_{off}^{app}) are obtained.

The inhibitors argatroban, efegatran, melagatran, NAPAP, CH 1091 and CH 248 also gave rise to linear dependence of the rate constants for approach to steady-state on the inhibitor concentrations. The apparent second-order rate constants for binding, (k_{on}^{app}) and the apparent first-order rate constants for dissociation (k_{off}^{app}) are summarised in Table I. From these values kinetically determined values for the dissociation constants K_i of the enzyme–inhibitor complex ($k_{off}^{app}/k_{on}^{app}$) are obtained, see Table I. The dependence of the final steady-state reaction rates on the concentration of the competitive inhibitor allows an independent calculation of the steady-state inhibition constants (K_i-values included in Table I), according to classical enzyme kinetics. The K_i-values obtained from the rate constants and those obtained from the steady-state rates are in good agreement.

Binding of Inhibitors Monitored by Changes in the Intrinsic Fluorescence of Thrombin

Although the results shown above demonstrate the usefulness of progress curve analysis on a fast time scale for monitoring the reaction rate, the

approach remains an indirect one and is limited to relatively slow rates of inhibitor binding. The use of stopped-flow spectrofluorimetry was therefore investigated to follow the reaction between inhibitors and thrombin. Recent work by Parry *et al.*[7] where changes in the intrinsic fluorescence of thrombin were found after binding of the inhibitor argatroban, used the same direct approach.

To investigate the possibility of using the intrinsic fluorescence of thrombin to monitor the binding of a variety of inhibitors, static fluorescence spectra of thrombin in the presence and absence of inhibitors were recorded with $\lambda_{ex} = 280$ nm. We found that all the inhibitors tested induced changes in the intrinsic fluorescence of thrombin. The relative fluorescence changes induced by the addition of inhibitors at concentrations well above their K_i values are summarised in the first column of Table II. The changes shown are all results of general increases or decreases in the quantum yield without changes in the position of the emission peak (340 nm) or the shape of the spectrum. Repeated additions of inhibitors did not produce any further changes in the fluorescence spectra. The largest relative fluorescence change (−25%) was found for argatroban, which is in good agreement with Parry *et al.*[7] The other compounds exhibited positive or negative changes in the range −26% to +10%. The (*R*)-epimer of CH 1091 at 2 μM produced a smaller fluorescence increase than was seen with the (*S*)-epimer, but in this case further additions of the ligand did result in additional changes. At a

TABLE II Kinetic parameters for inhibitor binding to thrombin obtained by stopped-flow spectrofluorimetry

Inhibitor	*Equilibrium fluorescence*[a] ΔF/F (%)	*Rate constants*		
		Fast component		*Slow component* k_{obs} (s^{-1})
		$k_{on}^{app} \times 10^{-7}$ ($M^{-1}s^{-1}$)	k_{off}^{app} (s^{-1})	
Argatroban	−26	5.3	32	33
NAPAP	−24[b]	2.1	23	9
Melagatran	−8	2.8	24	20
(*S*)-CH 1091	+10	1.6[c]	14	10
CH 248	+10	1.8[d]	—	6
Inogatran	+8	7.8[d]	—	27

[a] Change in fluorescence upon addition of 2 μM inhibitor to 0.2 μM thrombin in 0.05 M Hepes (pH 7.4) containing 0.1% PEG and 0.15 M with NaCl at 37°C.
[b] From reference [4].
[c] An 80/20 mixture of the *S*- and *R*-epimers was used.[11] The actual experimental value for the mixture was $k_{on}^{app} = 3.4 \times 10^6\ M^{-1}s^{-1}$. The value shown here was calculated assuming the *S*-isomer to be the active constituent.
[d] Initial slopes of the hyperbolic fits in Figure 5.

final concentration of 4 μM the fluorescence change was the same as that obtained with the *S*-epimer. This may originate from a small amount of contaminating (*S*)-CH 1091 in the preparation of (*R*)-1091 used.

When the reaction between thrombin and the inhibitors melagatran, NAPAP, CH 1091 and argatroban was studied with the stopped-flow apparatus using fluorescence detection, the time courses similar to that shown in Figure 3 for melagatran were obtained. Kinetic analysis of these traces showed that it was necessary to include two kinetic components in order to obtain a satisfactory fit. The slower component was, however, apparent only at low concentrations of the inhibitor, and accounted

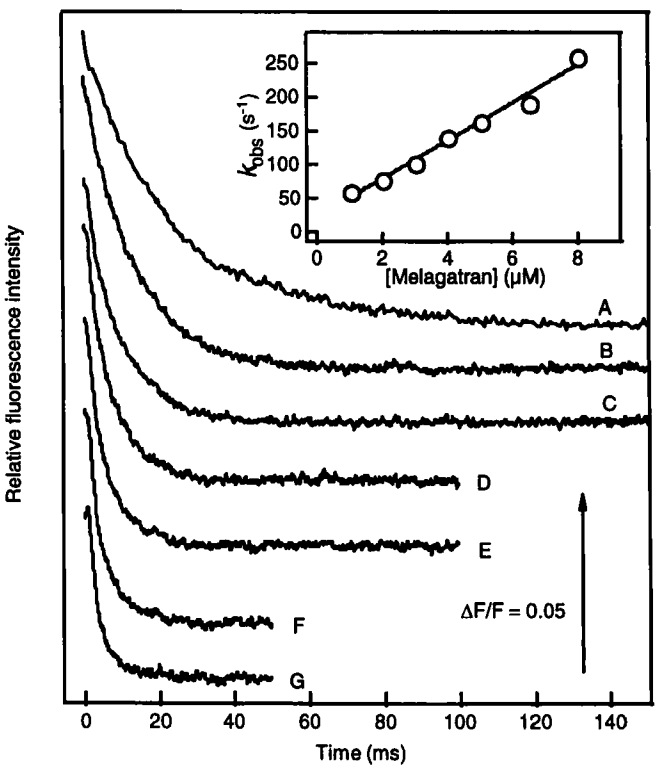

FIGURE 3 The reaction between melagatran and thrombin monitored using the intrinsic fluorescence of thrombin. Conditions were the same as in Figure 2, and the concentration of melagatran was: 1, 2, 3, 4, 5, 6.5 and 8 μM in curves A, B, C, D, E, F and G resp. The traces have been displaced vertically, showing only the first 150 ms of the reactions, but A, B and C were recorded to 500 ms, 200 ms and 200 ms, respectively. The inset shows the concentration dependence of the faster component of fluorescence decrease. The solid line with a slope of $28 \times 10^6\ M^{-1}\ s^{-1}$ and an ordinate intercept of $24\ s^{-1}$, was obtained by linear regression.

maximally for 10% of the total amplitude. The rate constant obtained for the faster component was found to be linearly dependent on the inhibitor concentration (inset in Figure 3), whereas little or no concentration dependence was found for the slower component. The slope and ordinate intercept obtained in this plot provide a second- and a first-order rate constant which, in the case of inhibitor binding in one step, correspond to the association and dissociation rate constants, respectively.[2,3] They will therefore be referred to as k_{on}^{app} and k_{off}^{app}. The apparent second- and first-order rate constants obtained from the slope and ordinate intercepts of such plots are summarised in Table II, together with the rate constant found for the slow component, when detectable. Moreover, when the reaction between the (*R*)-epimer of CH 1091 was investigated at a concentration of 2 μM, we found only a very slow reaction ($k_{obs} = 2\,s^{-1}$) associated with a much smaller change in fluorescence ($\Delta F/F = +3.7\%$) than that found with the *S*-epimer. This result is, again, consistent with the presence of a small amount of contaminating (*R*)-epimer, as also suggested from the static fluorescence.

It has been suggested that the binding of argatroban takes place in two steps, one step accompanied by a decrease in fluorescence, followed by a structural change in the protein, accompanied by an increase in fluorescence.[7] We have therefore also studied the reaction at very high concentrations of argatroban in an attempt to isolate a second step. Time courses obtained in this experiment are shown in Figure 4. The major part of the first kinetic component, associated with the decrease in fluorescence, now occurs in the dead time of the instrument, and only a small part of it is visible as a rapid initial decrease, followed by a much slower phase of fluorescence increase. For the latter reaction, a rate constant of $33\,s^{-1}$ was obtained, with an amplitude corresponding to a relative fluorescence increase of +3.6%. Attempts were also made to detect slower components in isolation, analogous to that seen with argatroban (Figure 4), using high concentrations of melagatran and CH 1091. However, only very small fluorescence changes were found ($|\Delta F/F| < 0.01$), and it was not possible to obtain a sufficient signal-to-noise ratio for kinetic analysis. This kind of experiment was not feasible with NAPAP due to its intrinsic fluorescence.[7]

Two kinetic components were found with both inogatran and with CH 248, with the slower components accounting for a small part of the total amplitude and not dependent on the inhibitor concentration. Figure 5 shows the time courses of the reaction between thrombin and inogatran. However, the concentration dependence of the rate constant for the faster components was not linear. This concentration dependence was found to

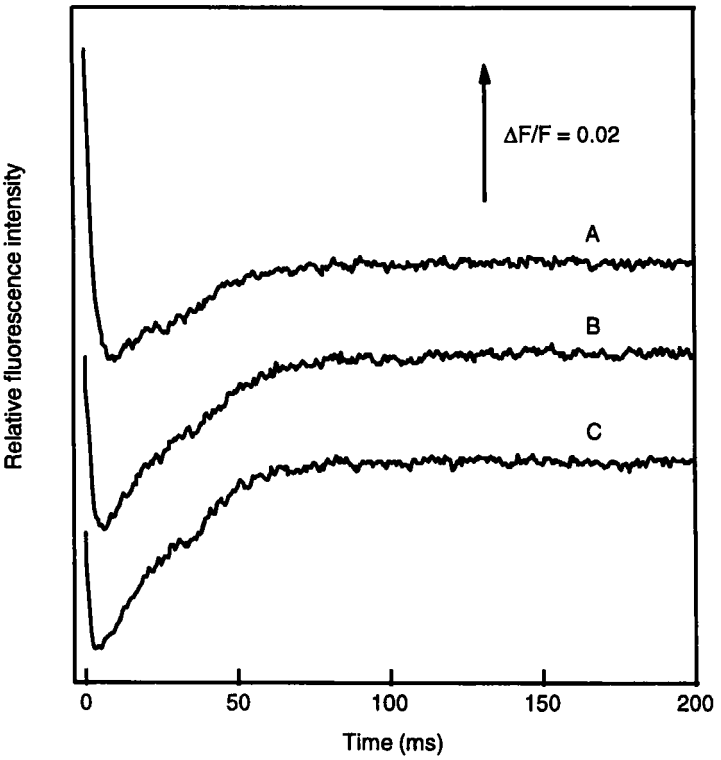

FIGURE 4 Time courses in the reaction between argatroban and thrombin at very high inhibitor concentrations. The concentration of thrombin after mixing was 0.38 μM. Conditions were the same as in Figure 2. The concentration of argatroban was: 20, 40 and 60 μM in trace A, B and C, respectively. The traces have been displaced vertically.

be satisfactorily described by a hyperbolic function:

$$k_{obs} = k \cdot k'^{*} \cdot [I]/(k + k' \cdot [I]), \qquad \text{(eq. 3)}$$

where k and k' are limiting first- and second-order rate constants, respectively. The solid lines in the figure shows the best fits of this general equation to the data, obtained with the parameters given in the figure legend. Attempts to isolate the slow component using high inhibitor concentrations were not successful, due to either an insufficient fluorescence change (inogatran) or too low a limiting value for the rate constant of the fast component (CH 248).

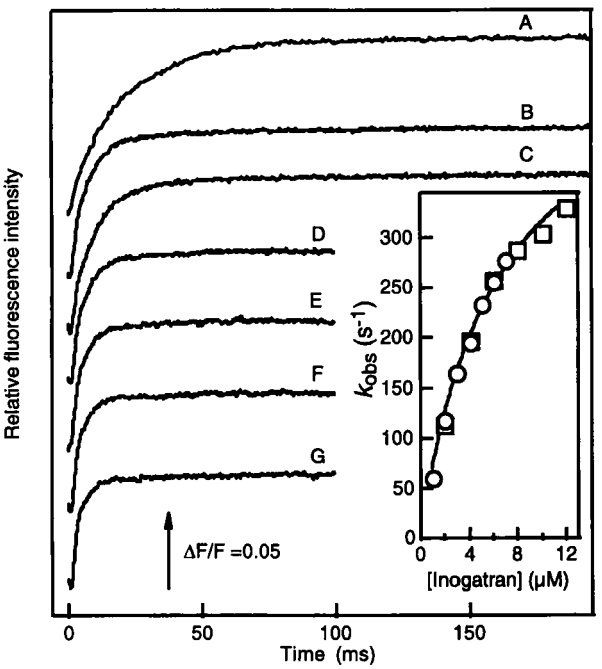

FIGURE 5 The reaction between inogatran and thrombin monitored using the intrinsic fluorescence of thrombin. Conditions were the same as in Figure 2, and the concentration of inogatran was: 1, 2, 3, 4, 5, 6 and 7 μM in A, B, C, D, E, F and G, respectively. The traces have been displaced vertically and were recorded to 200 ms. The inset shows the concentration dependence of the faster component of fluorescence increase. The solid line shows the best fit of a hyperbolic function to the experimental data, obtained with a limiting first-order rate constant of $67\,s^{-1}$ at high concentration and a limiting second-order rate constant, $18 \times 10^6\,M^{-1}\,s^{-1}$ at low concentration of inogatran.

DISCUSSION

The rate of binding of different types of inhibitors to human thrombin has been studied here using two different approaches. In progress curve analysis, binding is monitored through the onset of inhibition, whereas changes in the intrinsic fluorescence is a more direct measure of ligand binding to the enzyme. As seen in Table II, the two methods give reasonably consistent values for the second-order rate constant for inhibitor binding. The values obtained with the fluorescence method are, however, slightly, but consistently, larger than those obtained by progress curve analysis. A more pronounced difference is seen when comparing the k_{off} values. The compounds that exhibited a linear concentration dependence of the faster component (argatroban, melagatran, NAPAP and (*S*)-CH 1091) exhibited

a substantially higher value for the k_{off}^{app} by the fluorescence method than the values obtained from progress curve analysis. These differences are not expected if inhibitor binding and inhibition takes place in a single step, and indicate a more complex mode of interaction of thrombin and these inhibitors, consistent with the multiple phases observed when inhibitor binding was monitored through fluorescence changes.

The presence of a structural change on the route to the final thrombin–inhibitor complex has been suggested earlier.[7,12–14] The present finding that a slow kinetic component can be isolated, associated with a fluorescence change with the opposite sign of that associated with binding, strongly supports a structural change.

In the light of the above considerations, a minimal kinetic mechanism for inhibitor binding would be a two-step reaction:

$$E + I \underset{k_{-1}}{\overset{k_1}{\rightleftharpoons}} EI_1 \underset{k_{-2}}{\overset{k_2}{\rightleftharpoons}} EI_2 \qquad \text{(Scheme 1)}$$

This mechanism would give rise to two apparent rate constants, as observed. When the first reaction is much faster than the second, using relatively high concentrations of inhibitors, the relaxation of the first and second equilibria takes place on sufficiently different time scales as not to interfere with each other. The observed fast and slow kinetic components would then reflect the relaxation of the first and second step, respectively. However, the hyperbolic concentration dependence found for the fast component with CH 248 and inogatran (Figure 5) suggests that the situation is more complex. It has been pointed out by Fersht[15] that the observed behaviour is common when a binding reaction takes place in two steps, with a high dissociation constant for the first step. The overall process of inhibitor binding may actually take place in three steps:

$$E + I \underset{k_{-1}}{\overset{k_1}{\rightleftharpoons}} EI_0 \underset{k'_{-1}}{\overset{k'_1}{\rightleftharpoons}} EI_1 \underset{k_{-2}}{\overset{k_2}{\rightleftharpoons}} EI_2 \qquad \text{(Scheme 2)}$$

Although a hyperbolic concentration dependence was observed only for two of the compounds investigated, it is reasonable to assume that all the compounds investigated bind by a similar route. In this case, the first step would be entirely rate-limiting in the initial binding of argatroban, NAPAP,

CH 1091 and melagatran, whereas the second step becomes partially rate-limiting for initial binding at the high concentrations of inogatran and CH 248. Under the conditions used the first two steps take place on a much faster time scale than the third. When the first step is faster than the second, the apparent rate constants for binding then become:

$$\frac{1}{\tau_1} = k_1[\mathrm{I}] + k_{-1}; \quad \frac{1}{\tau_2} = k'_{-1} + \frac{k'_1[\mathrm{I}]}{\frac{k+k'_1}{k_1} + [\mathrm{I}]}. \qquad \text{(eq. 4)}$$

The hyperbolic dependence observed with inogatran and CH 248 suggests that the fast kinetic component observed here reflects $1/\tau_2$, if the change in fluorescence is associated mainly with the second step. The linear concentration dependence seen with the other compounds arises if $k_{-1}/k_1 \gg [\mathrm{I}]$ throughout the concentration range. In this case, the apparent second-order rate constant k_{on}^{app} obtained from the slopes of the straight line in Figure 3, or the initial slopes of the hyperbolas in Figure 5 thus becomes:

$$k_{on}^{app} = \frac{k_1 k'_1}{k_{-1} + k'_1}, \qquad \text{(eq. 5)}$$

whereas the ordinate intercept reflects the rate constant for the reverse reaction in the second step, k'_{-1}. This reaction thus appears much faster for the compounds with linear concentration dependence than in inogatran and CH 248. When E, EI_0 and EI_1 are at equilibrium, the third step then gives rise to the observed slow kinetic component with an apparent rate constant given by k_2 multiplied by the fraction of EI_1 present.

It is of interest to examine if the different rate constants obtained with progress curve analysis and the fluorescence method are consistent with Scheme 1. In the former experiments, substrate is present in large excess over inhibitor. This effectively slows down the forward reaction in the binding step, and its effective rate constant is now expected to become the smallest of the microscopic rate constants. Under these conditions, the second step is much faster than the first step and is at equilibrium. Moreover, the first step is expected to be faster than the third due to a high value of k_{-1}. These conditions are expected[15] to result in two kinetic components that are linearly dependent on the inhibitor concentration:

$$\text{(a)}\ \frac{1}{\tau_1} = k_1[\mathrm{I}] + k_{-1}(1 - \alpha(\mathrm{EI}_1)) \quad \text{and} \quad \text{(b)}\ \frac{1}{\tau_2} = \frac{k_1 k_2 \alpha(\mathrm{EI}_1)[\mathrm{I}]}{k_{-1}(1 - \alpha(\mathrm{EI}_1))} + k_{-2}, \qquad \text{(eq. 6)}$$

where $\alpha(EI_1)$ is the fraction of EI_1 present when EI_1 and EI_0 are at equilibrium. The values found for the apparent second-order rate constants by progress analysis are consistently smaller than those obtained with the fluorescence assay (Table II). This suggests that the onset of inhibition under the conditions in the progress curve experiments takes place at the rate given by the slower component in equation (6b). In this case the first- and second-order rate constants, obtained from the concentration dependence of the observed rate constant, become:

$$\text{(a) } k_{on}^{app} = \frac{k_1 k_1' k_2}{k_{-1} k_{-1}'} \quad \text{and} \quad \text{(b) } k_{off}^{app} = k_{-2}. \qquad \text{(eq. 7)}$$

The different values of k_{off}^{app} and k_{on}^{app} obtained by the fluorescence and progress curve methods (Table II) can thus be seen as consequences of the stepwise character of the reaction, together with the widely different rates of initial inhibitor binding in the two experimental systems.

The microscopic rate constants in Scheme 2 are related to the steady-state K_i value through:

$$K_i = \frac{1}{\frac{k_1}{k_{-1}} + \frac{k_1 k_1'}{k_{-1} k_{-1}'} + \frac{k_1 k_1' k_2}{k_{-1} k_{-1}' k_{-2}}}. \qquad \text{(eq. 8)}$$

A comparison with equation 5 shows good correspondence between the experimental steady-state K_i values and those obtained from progress curve analysis calculated from $k_{off}^{app}/k_{on}^{app}$. This is consistent with the equilibrium position of the third step, being strongly shifted towards EI_2. It is therefore likely that this step makes a major contribution to the overall thermodynamics of inhibitor binding. Furthermore, at a low inhibitor concentration, the intermediates EI_0 and EI_1 will not accumulate under the conditions used in progress curve analysis. In this case, the same apparent rate constants will be obtained for inhibitor binding and for dissociation of the enzyme–inhibitor complex, as observed.

The recent studies by Parry *et al.*[7] show that the susceptibility of thrombin to limited proteolysis was decreased considerably in the presence of both the reversible inhibitor argatroban and of the irreversible inhibitor D-Phe-Pro-Arg-CH_2Cl (PPACK). These results suggest structural differences, particularly in the so-called 149 insertion loop[14], between unliganded and inhibited thrombin. A possible origin of the slow kinetic component of inhibitor binding found in the present work is therefore rearrangement of this part of thrombin after the initial binding of inhibitor, with stronger

protein–ligand interactions as the result. The overall affinity of thrombin for an inhibitor is, in this case, determined by interactions between the inhibitor and the protein in its inhibited conformation. On the other hand, at inhibitor concentrations in the nanomolar range, the rate of binding will be determined by the forward rate constant for the structural change (k_2), together with the equilibrium constants for the two first steps (equation 7a). The rate of binding will therefore in this case be influenced by the thermodynamics of interaction between the inhibitor and the enzyme in its uninhibited conformation. Both fast and tight binding, are important objectives in the design of therapeutic thrombin inhibitors. The present results suggest that the thermodynamics of interaction between inhibitors and thrombin in its uninhibited conformation could be useful as a design criterion for fast-binding thrombin inhibitors.

References

[1] Stone, A.R. and Tapparelli, C. (1995). *J. Enzym. Inhib.*, **9**, 3.
[2] Morrisson, J.F. and Walsh, C.T. (1987). *Adv. Enzymol. Relat. Areas Mol. Binding*, **61**, 201.
[3] Cha, S. (1976). *Biochem. Pharmacol.*, **24**, 2177.
[4] Lewis, S.D., Ng, A.S., Baldwin, J.J., Fusetani, N., Naylor, A.M. and Shafer, J.A. (1993). *Thromb. Res.*, **70**, 173.
[5] Kettner, C., Mersinger, L. and Knabb, R. (1990). *J. Biol. Chem.*, **265**, 18289.
[6] Gutheil, W.G. and Bachovchin, W.W. (1993). *Biochemistry*, **32**, 8723.
[7] Parry, M.A.A., Stone, S.R., Hofsteenge, J. and Jackman, M.P. (1993). *Biochem. J.*, **290**, 665.
[8] Lottenberg, R., Hall, J.A., Blinder, M., Binder, E.P. and Jackson, C.M. (1983). *Biochim. Biophys. Acta*, **742**, 359.
[9] Di Cera, E., De Cristofaro, R., Albright, D.J. and Fenton, J.W. (1991). *Biochemistry*, **30**, 7913.
[10] Sjöling, Å. (1992). *Diploma thesis*, Dept. Biochemistry and Biophysics, Göteborg University and Chalmers University of Technology.
[11] Jones, D.M., Atrash, B., Teger-Nilsson, A.C., Gyzander, E., Deinum, J. and Szelke, M. (1995). *Proceedings of the 23rd European Peptide Symposium* (Maia, H.L.S., ed.), ESCOM Leiden, pp. 899–900.
[12] De Cristofaro, R. and Landolfi, R. (1994). *J. Mol. Biol.*, **239**, 569.
[13] Nienaber, V.I., Mersinger, L.J. and Kettner, C.A. (1996). *Biochemistry*, **35**, 9690.
[14] Engh, R.A., Brandstetter, H., Sucher, G., Eichinger, A., Baumann, U., Bode, W., Huber, R., Poll, T., Rudolph, R. and von der Saal, W. (1996). *Structure*, **4**, 1353.
[15] Fersht, A. (1985). In *Enzyme Structure and Mechanism*, 2nd ed, pp. 133–143. New York, USA: W.H. Freeman & Co.